



Connecting Inflation to the NANOGrav 15-year Data Set via Massive Gravity

Ved Kenjale ^{1,*} and Tina Kahniashvili ^{1,2,3,†}

¹*McWilliams Center for Cosmology and Astrophysics and Department of Physics,
Carnegie Mellon University, Pittsburgh, Pennsylvania 15213, USA*

²*School of Natural Sciences and Medicine, Ilia State University, 0194 Tbilisi, Georgia*

³*Abastumani Astrophysical Observatory, Tbilisi GE-0179, Georgia*

(Dated: October 15, 2024)

Several pulsar timing array (PTA) missions have reported convincing evidence of a stochastic gravitational wave background within their latest datasets. This background could originate from an astrophysical source, though there are multiple possibilities for its origin to be cosmological. Focusing on the NANOGrav signal, which was in good agreement with other PTAs, we evaluate the possibility of an inflationary source for the background. However, we'll consider a time-dependent minimal theory of massive gravity instead of standard general relativity for our analysis. We find that an inflationary interpretation will require a strongly blue spectrum, characterized by $n_T = 1.8 \pm 0.54$, while Big Bang Nucleosynthesis limits will require a low reheating scale of $T_{\text{rh}} \simeq 4000$ GeV. Though these constraints make it difficult for inflation to be the source of the NANOGrav signal, we find that the massive gravity model allows for a greater reheating temperature than standard general relativity, making an inflationary interpretation slightly less cumbersome.

I. INTRODUCTION

Inflation has become the widely accepted model for describing the evolution of the early universe [1–3]. The inflationary paradigm solves the horizon, flatness, and magnetic monopole (non-existence) problems, and produces a stochastic background of relic gravitational waves (GWs) via parametric amplification of zero-point quantum-mechanical fluctuations in the gravitational field [1, 4] (see [5] for a review). There has yet to be a detection of relic GWs, but such an event could confirm inflation, test fundamental physics, and provide unique insight into the characteristics of the very early universe prior to recombination [6]. An avenue for the detection of primordial GWs lies in pulsar timing arrays (PTAs), which utilize millisecond pulsars as stable clocks [7]. GWs perturb the space-time along the line-of-sight to a pulsar, causing spatially correlated fluctuations to manifest in the arrival time of pulses [8, 9].

Recently, the North American Nanohertz Observatory for Gravitational Waves (NANOGrav) [10], the European Pulsar Timing Array (EPTA) [11–13], the Parkes Pulsar Timing Array (PPTA) [14, 15], and the Chinese Pulsar Timing Array (CPTA) [16] collaborations released analyses of their newest PTA datasets. Their analyses show evidence of the Hellings-Downs correlations [17], which indicate a true GW source for the observed PTA signal and supports the existence of a stochastic GW background [18]. These datasets will also allow us to test fundamental physics, including general relativity (GR) (see Ref. [19] for a living review). For the rest of this work, we will consider the NANOGrav 15-year dataset [20].

The detection of a stochastic GW background via PTAs could be understood as a signal from the early universe, though a component of this signal may arise from astrophysical sources [21, 22]. Previous works [23–40] have investigated an interpretation of the NANOGrav signals (the NANOGrav 15-year dataset [20] and/or the previous NANOGrav 12.5-year dataset [41]) assuming GWs generated by inflation. These works found that a strongly blue spectrum and a low reheating temperature would be needed to interpret the PTA signal as inflationary GWs; hence, inflationary models past the simplest ones would be required. One possibility for modifying the inflationary paradigm is to relax the assumption of GR as the true theory of gravity (at all energy and length scales).¹ Our goal is to determine if modifications to GR would result in a more feasible interpretation of inflationary GWs as a source for the PTA signals. In particular, we'll focus on a theory known as massive gravity (MG), where the graviton has a non-zero mass m [43].

The theory of MG was pioneered by Fierz and Pauli in 1939, as they considered the addition of a Lorentz-invariant mass term to a linearized spin-2 field [44]. MG has become quite relevant during the last few decades due to the accelerated expansion of the universe today, which can be explained by a graviton mass term without the need for dark energy or the presence of a cosmological constant [45]. For quite some time, a modification to the nil graviton mass proved to be difficult. Linear theories of MG fail to reduce to GR in the massless graviton limit, due to the van Dam-Veltman-Zakharov (DVZ) discontinuity [46, 47].² Non-linear theories have also been considered: the non-linear extension to Fierz-Pauli MG

* vedk@cmu.edu

† tinatin@andrew.cmu.edu

¹ Inflationary models, and their characteristics, are constrained through the Cosmic Microwave Background (CMB) anisotropies [42].

² Theories of MG have five polarization modes: in addition to the

is subject to the Vainshtein screening mechanism [48], which removes additional polarization modes. However, the theory still suffers from ghost degrees of freedom: a helicity-0 mode in the gravity sector may be absent at the quadratic order of Fierz-Pauli MG but revive at a higher order, acting as a ghost [49].

A more recent effort resulted in the breakthrough formulation of a ghost-free MG model: deRham-Gabadadze-Tolley (dRGT) [50, 51], and its bigravity generalization [52]. These formulations of viable MG models have led to investigations on the effect of a non-zero graviton mass on GW generation and propagation - see Refs. [53, 54] for pioneering works, and Ref. [55] for a review. Another option for avoiding the Boulware-Deser ghost is by relaxing the necessity for Lorentz-invariance [56–59]. Then, the massive graviton forms a representation of a 3D rotation group, instead of the 4D Lorentz group it would form with Lorentz-invariance. As a result of this, the number of degrees of freedom in the gravity sector is no longer forced to be five.

The minimal theory of MG (MTMG) is a model that utilizes this, retaining only two degrees of freedom in the gravity sector, from the two tensor modes [60, 61]. Lorentz-violating theories, like MTMG, also avoid the Higuchi bound, which requires that the Lorentz-invariant graviton mass should be greater than the Hubble expansion rate by a factor up to order unity to avoid turning extra degrees of freedom into ghosts in cosmological backgrounds [62].

This work will utilize a time-dependent MTMG, with the graviton mass following a step function as in Ref. [63]. We will evaluate how MTMG can affect the inflationary interpretation of the NANOGrav 15-year dataset. The paper is organized as follows: in Section II, we review the models for inflationary GWs, MG, and PTA data. In Section III, we connect PTA data and inflation using transfer functions. In Section IV, we map our results to the inflationary regime, and explore the implications of this in Section V. We conclude and discuss future extensions in Section VI. We will use natural units with $c = \hbar = k_B = 1$. We set the present day Hubble parameter to $H_0 = 100h_0 \text{ km s}^{-1} \text{ Mpc}^{-1} = 67.66 \text{ km s}^{-1} \text{ Mpc}^{-1}$, noting that this value isn't a universal constant due to the Hubble tension [64]. We set the present day radiation, matter, and dark energy density parameters to $\Omega_R, \Omega_M, \Omega_\Lambda = 9.182 \times 10^{-5}, 0.3111, 0.6889$ using *Planck* 2018 data [64].

II. MODEL SETUP

We begin by defining the line element of the Friedmann–Lemaître–Robertson–Walker (FLRW) flat metric:

$$ds^2 = a^2(\tau) \left[-d\tau^2 + (\delta_{ij} + h_{ij}) dx^i dx^j \right], \quad (1)$$

where $a(\tau)$ and τ denote the scale factor and conformal time respectively, and h_{ij} denotes the traceless and transverse (i.e. $g^{ij}h_{ij} = \partial_i h_{ij} = 0$) tensor perturbation to flat space. Going into momentum space, we decompose the tensor perturbation h_{ij} into its helicity states (see Eq. 19.214 of [5]):

$$h_{ij}(\tau, \mathbf{k}) = \sum_{\lambda=+,\times} e_{ij}^\lambda(\mathbf{k}) h_k^\lambda(\tau, \mathbf{k}), \quad (2)$$

where \mathbf{k} is the comoving momentum, $+$ and \times denote the two polarization states, and e_{ij}^λ are the polarization tensors defined by (see Eqs. 19.216–217 of [5]):

$$e_{ij}^+(\hat{\mathbf{k}}) = \hat{\mathbf{u}}_i \hat{\mathbf{u}}_j - \hat{\mathbf{v}}_i \hat{\mathbf{v}}_j \quad (3)$$

$$e_{ij}^\times(\hat{\mathbf{k}}) = \hat{\mathbf{u}}_i \hat{\mathbf{v}}_j - \hat{\mathbf{v}}_i \hat{\mathbf{u}}_j. \quad (4)$$

The unit vectors $\hat{\mathbf{u}}$ and $\hat{\mathbf{v}}$ are orthogonal to each other and $\hat{\mathbf{k}}$, and the polarization tensors are also normalized as:

$$e_{ij}^\lambda(\hat{\mathbf{k}}) e_{ij}^{\lambda'}(\hat{\mathbf{k}}) = 2\delta^{\lambda\lambda'}. \quad (5)$$

We now introduce the relevant equations for MTMG. First, the general quadratic action is given by [54, 60, 61, 63, 65]:

$$S = \frac{M_{\text{Pl}}^2}{8} \int d\tau d^3x a^2 \left[(h'_{ij})^2 - (\partial h_{ij})^2 - a^2 M_{\text{gw}}^2 h_{ij}^2 \right], \quad (6)$$

where M_{Pl} is the Planck mass, M_{gw} is the graviton mass³, and the primes ($'$) denote derivatives with respect to the conformal time τ . The graviton mass will follow a step function, given by:

$$M_{\text{gw}}(\tau) = \begin{cases} m & \tau < \tau_m \\ 0 & \tau > \tau_m \end{cases}, \quad (7)$$

where τ_m , the cutoff time, denotes the conformal time at which the graviton mass drops to nil. Though this instantaneous change to zero in the graviton mass is somewhat unphysical, specifying an exact form of this function would require fixing a model that incorporates the dynamics of other fields. However, the overarching effect of a time-dependent theory of MG can still be studied using the simple step function mass, while taking advantage of

regular tensor (spin ± 2) modes, there are scalar (spin 0) and vector (spin ± 1) modes that do not disappear in the $m \rightarrow 0$ limit, i.e. regular GR is not recovered.

³ The graviton mass and the mass of GWs may differ in some scenarios, see Refs. [66–72] for examples using a quasidilaton theory of MG.

the simplified analytical and numerical calculations permitted. Since we will also be considering GR, we note that $M_{\text{gw}} = 0$ for GR.

Following the standard procedure of minimizing the action, Eq. 6, and utilizing the helicity decomposition from Eq. 2, we obtain the equation of motion (EoM) for h_k [54, 63]:

$$\bar{h}_k'' + \left(k^2 + a^2 M_{\text{gw}}^2 - \frac{a''}{a} \right) \bar{h}_k = 0, \quad (8)$$

where $\bar{h}_k = a \cdot h_k$, and we've suppressed the subscript λ on h_k^λ denoting the polarization mode since the two polarization modes follow the same EoM (i.e. unpolarized GWs). From the EoM, we also acquire the dispersion relation:

$$\omega^2 = \frac{k^2}{a^2} + M_{\text{gw}}^2, \quad (9)$$

which relates the frequency ω to the wavenumber k ⁴. From an initial conformal time τ_i , a mode h_k will evolve according to Eq. 8, which we summarize via the transfer function:

$$\mathcal{T}(\tau, k) = \frac{h_k(\tau)}{h_k(\tau_i)}. \quad (10)$$

To characterize the GW signal, we define the tensor power spectrum as:

$$\mathcal{P}_T(\tau, k) \equiv \frac{k^3}{\pi^2} \sum_{\lambda=+, \times} |h_k^\lambda(\tau)|^2 = \frac{2k^3}{\pi^2} |h_k(\tau)|^2. \quad (11)$$

We can recast this in terms of the transfer function by first defining the primordial tensor power spectrum: $\mathcal{P}_T^{\text{prim}}(k) \equiv \mathcal{P}_T(\tau_i, k)$. It follows that:

$$\mathcal{P}_T(\tau, k) = \mathcal{P}_T^{\text{prim}}(k) \mathcal{T}^2(\tau, k). \quad (12)$$

The relevant quantity for GW detection experiments is the GW spectral energy density, Ω_{gw} , a dimensionless quantity that describes the strength of GWs in terms of their energy density. It is given by the logarithmic derivative with respect to wavenumber of the GW energy density ρ_{gw} , divided by the critical density ρ_c [79], and is evaluated at a conformal time τ :

$$\Omega_{\text{gw}}(\tau, k) \equiv \frac{1}{\rho_c} \frac{d\rho_{\text{gw}}}{d \ln k}. \quad (13)$$

This can be defined in terms of the transfer function by first identifying ρ_{gw} as the 00-component of the energy-momentum tensor $T^{\mu\nu}$ [80]:

$$T^{00} = \rho_{\text{gw}} = \frac{1}{64\pi G a^2} \langle (\partial_\tau h_{ij})^2 + (\vec{\nabla} h_{ij})^2 \rangle \quad (14)$$

$$= \frac{1}{32\pi G} \int \frac{d^3k}{(2\pi)^3} \frac{k^2}{a^2} \cdot 2 \sum_{\lambda=+, \times} |h_k^\lambda|^2, \quad (15)$$

Substituting this into Eq. 13 yields the desired form [81, 82]:

$$\Omega_{\text{gw}}(k) = \frac{k^2}{12H_0} \mathcal{T}^2(\tau_0, k) \mathcal{P}_T^{\text{prim}}(k), \quad (16)$$

where we've evaluated the expression at $\tau = \tau_0$. This form of the GW spectral energy density is useful since it contains two distinct factors: the transfer function, $\mathcal{T}(\tau_0, k)$ and the primordial tensor power spectrum $\mathcal{P}_T^{\text{prim}}(k)$. Let's set the initial conformal time τ_i from which the transfer function is defined by to the conformal time at which inflation ends. Then, $\mathcal{P}_T^{\text{prim}}(k)$ gives the tensor power spectrum at the end of inflation. This also means that $\mathcal{T}(\tau_0, k)$ represents the evolution of a GW mode in the universe from the end of inflation till the present time. Hence, this definition of τ_i has effectively split the GW spectral energy density into a part dependent on inflation, and by extension a particular inflationary model, and a part independent of inflation. This latter part, $\mathcal{T}(\tau_0, k)$, is governed by Eq. 8 and thus depends on the model of gravity being considered.

The specific form of the transfer function $\mathcal{T}(\tau_0, k)$ will be discussed later, but to connect to inflation, we must specify the form of the primordial tensor power spectrum $\mathcal{P}_T^{\text{prim}}(k)$. Since we will eventually constrain the inflationary period via the NANOGrav signal, we approximate the primordial tensor power spectrum as a power-law, as is convention [5]:

$$\mathcal{P}_T^{\text{prim}}(k) = r A_s \left(\frac{k}{k_\star} \right)^{n_T}, \quad (17)$$

where r denotes the tensor-to-scalar ratio, A_s is the amplitude of primordial scalar perturbations at the CMB pivot scale k_\star , chosen as $k_\star = 0.05 \text{ Mpc}^{-1}$ in this work to match *Planck* 2018 [64], and n_T is the tensor spectral index. If $n_T = 0$, the spectrum is scale-invariant (no dependence on k), while $n_T < 0$ is called as a red spectrum and $n_T > 0$ is called a blue spectrum. The single-field slow-roll inflationary model adheres to a ‘‘consistency relation’’ given by $n_T = -r/8$ [83], which would imply a red spectrum for this model given that $r > 0$. The spectral index n_T is also related to the equation-of-state w for the dominant component during the inflationary period by [5]:

$$n_T = \frac{4}{1 + 3w} + 2. \quad (18)$$

⁴ The first and third GW Transient Catalogs (GWTC-1 and GWTC-3) enabled the search for cosmic strings, and can probe the graviton mass at scales around 10^{-23} eV [73, 74]. PTA dataset analysis has constrained this to about $3.8 \times 10^{-23} \text{ eV}$ [75, 76]. CMB and baryon acoustic oscillations further constrain the graviton mass in extended MTMG to around $6.6 \times 10^{-34} \text{ eV}$ [77, 78].

An inflationary period characterized by de Sitter expansion would have $w = -1$, and thus $n_T = 0$ for a scale-invariant spectrum. For simple scalar-field inflationary models (including single-field slow-roll inflation), we have $w > -1$, yielding a slightly red spectrum with $n_T < 0$ [3]. For phantom inflationary models, we have $w < -1$ and thus $n_T > 0$, i.e. a blue spectrum [84]. It is also important to note that the constraint $w < -1/3$ (see Section 17.2 of Ref. [5]), needed for the universe to follow an accelerating expansion during inflation, implies that $n_T < 2$.

As mentioned previously, we will utilize the GW spectral energy density to connect our model to an observed signal (i.e. NANOGrav 15-year dataset). For a PTA signal, this is typically given as:

$$\Omega_{\text{gw}}^{\text{PTA}}(f) = \frac{2\pi^2}{3H_0^2} f^2 h_c^2(f), \quad (19)$$

where $h_c(f)$ is the power spectrum of the GW strain, approximated as the power law:

$$h_c(f) = A \left(\frac{f}{f_{\text{yr}}} \right)^\alpha, \quad (20)$$

where A is the intrinsic-noise amplitude, the reference frequency $f_{\text{yr}} = 1 \text{ yr}^{-1}$, and the spectral index α is given by:

$$\alpha = \frac{3 - \gamma}{2}, \quad (21)$$

where γ is spectral index for the pulsar timing residual cross-power spectral density $S(f) \propto f^{-\gamma}$ [20]. Using Eqs. 19, 20, and 21 we can express the GW spectral energy density for a PTA signal as:

$$\Omega_{\text{gw}}^{\text{PTA}}(f) = A^2 \frac{2\pi^2}{3H_0^2} \frac{f^{5-\gamma}}{\text{yr}^{\gamma-3}}. \quad (22)$$

The intrinsic-noise amplitude A and the spectral index γ are used to characterize the results of PTA GW experiments. The NANOGrav collaboration reports their results as joint A - γ posteriors or posteriors for A at a fixed value of γ , often $\gamma = 13/3$ (the expected value of γ for a stochastic GW background originating from supermassive black hole binaries (SMBHBs)) [20]. We shall utilize the joint A - γ posteriors in Section IV.

III. TRANSFER FUNCTIONS

In this section, we work towards numerically integrating the EoM (Eq. 8) to calculate the transfer function $\mathcal{T}(\tau_0, k)$ (Eq. 10) in the GR and MG paradigms. These transfer functions will then be used to calculate the GW spectral energy density (Eq. 16) before connecting to PTA data.

The form of the EoM requires that we specify the graviton mass M_{gw} and the scale factor a as functions

of conformal time, over the relevant time domain. In our case, we will integrate (over conformal time) from the end of inflation to the present day, and we'll use $\tau_0 = 1.375 \times 10^4 \text{ Mpc}$ (see. Eq. 17.168 of [5]). The functional form for the graviton mass was given in Eq. 7, but the non-zero mass m and the cutoff time τ_m must be specified. The present day graviton mass is bounded by the relation $M_{\text{gw}} \lesssim 2 \times 10^{-28} \text{ eV}/c^2$ from the orbital decay of binary pulsars [85, 86], but since we are considering a step function mass, it's not necessary to follow this constraint. We choose $m = 10^9 \cdot H_0$ to match Refs. [54, 63], though we note that this choice is somewhat arbitrary. As for the cutoff time, the binary neutron star merger labeled as events GW170817 and GRB170817A occurred at $z \simeq 10^{-2}$ and bounded the propagation speed of gravitons [87]. However, we choose to conservatively assume that the cutoff time occurs around the matter-radiation equality. This choice will also simplify the numerical simulation, as only part of the matter dominated era will have a non-zero graviton mass. In particular, we choose:

$$\tau_m = 5\tau_{\text{eq}} \quad (23)$$

$$= 5(\sqrt{2} - 1)\tau_\star \quad (24)$$

$$= 5(\sqrt{2} - 1) \frac{2\Omega_R^{1/2}}{H_0\Omega_M}, \quad (25)$$

where τ_{eq} is the conformal time at matter-radiation equality, τ_\star is a conformal time scale, and the last two lines come from Eqs. 17.153-154 of [5]. For the scale factor, we'll use:

$$a(\tau) = a_{\text{eq}} \left[\frac{2\tau}{\tau_\star} + \left(\frac{\tau}{\tau_\star} \right)^2 \right], \quad (26)$$

which holds during the radiation dominated and matter dominated epochs (see Eq. 17.152 of [5]). We do not explicitly consider a dark energy dominated era, but the effects of this era will be included as an additional factor in the transfer function. This factor is approximated as [88, 89]:

$$\mathcal{T}_2 = \frac{\Omega_M}{\Omega_\Lambda} \simeq 0.451, \quad (27)$$

using the values previously defined for Ω_M and Ω_Λ . Another effect to note is the damping caused by free-streaming neutrinos from decoupling in the early universe. This free-streaming produces an anisotropic stress [90], which can reduce the amplitude of modes that enter the horizon during the radiation dominated era [91]. Defining \mathcal{T}_3 to be the factor associated with neutrino free-streaming, we have:

$$\mathcal{T} = \mathcal{T}_1 \cdot \mathcal{T}_2 \cdot \mathcal{T}_3, \quad (28)$$

where \mathcal{T}_1 is the contribution from the numerical integration of the EoM.

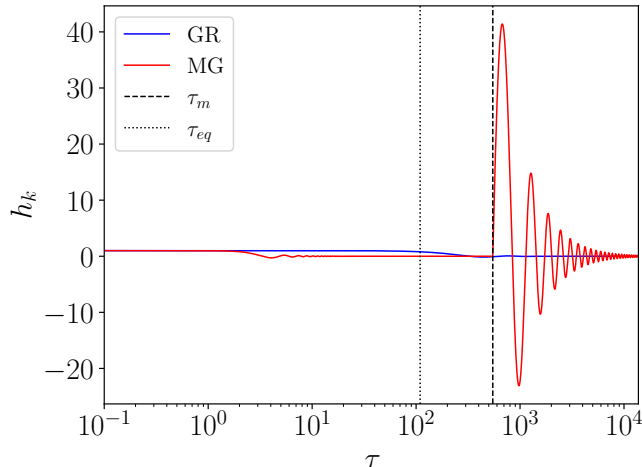


FIG. 1. Evolution of the mode $k = k_{\text{eq}}$ in the GR and MG models, where $k_{\text{eq}} = 0.010339 \text{ Mpc}^{-1}$ is the wavenumber for a mode crossing the horizon at matter-radiation equality [64]. This simulation assumes $h_k = 1$ prior to the mode entering the horizon. Observe that in the GR case, the mode does enter the horizon at $\tau = \tau_{\text{eq}}$, where τ_{eq} is the conformal time of horizon reentry for k_{eq} (note the logarithmic scale for τ).

With the graviton mass M_{gw} and the scale factor a specified, we now proceed with the numerical integration of the EoM. The evolution of a single mode in the GR and MG paradigms is shown in Fig. 1. We repeat this integration for a domain of k values, allowing us to calculate the transfer functions in the GR and MG cases:

$$\mathcal{T}_1^{\text{GR}}(k) = \frac{3j_1(k\tau_0)}{k\tau_0} \sqrt{0.96 + 0.97 \left(\frac{k}{k_{\text{eq}}}\right) + 4.16 \left(\frac{k}{k_{\text{eq}}}\right)^2} \quad (29)$$

$$\mathcal{T}_1^{\text{MG}}(k) = \frac{3j_1(k\tau_0)}{k\tau_0} \cdot \sqrt{2.1 \cdot 10^4 + 5.8 \cdot 10^4 \left(\frac{k}{k_{\text{eq}}}\right) + 1.3 \cdot 10^6 \left(\frac{k}{k_{\text{eq}}}\right)^2}, \quad (30)$$

where j_1 is the first spherical Bessel function, given by $j_1(x) = \sin(x)/x^2 - \cos(x)/x$. The GR transfer function has good agreement with previous works, which found similar coefficients [89, 92]. Since the GR and MG case transfer functions have the same functional form (which was utilized to perform function fitting to obtain the coefficients shown in Eqs. 29 and 30), we'll simply use:

$$\mathcal{T}_1(k) = \frac{3j_1(k\tau_0)}{k\tau_0} \sqrt{s_3 + s_2 \left(\frac{k}{k_{\text{eq}}}\right) + s_1 \left(\frac{k}{k_{\text{eq}}}\right)^2}, \quad (31)$$

and insert the appropriate values of s_1, s_2 , and s_3 when necessary. Note that the NANOGrav PTA signal occurs at $f \sim 10^{-9} \text{ Hz}$, which corresponds to $k \sim 10^6 \text{ Mpc}^{-1}$. Since this scale is much greater than k_{eq} , we can simplify

Eq. 31 by working in the $k \gg k_{\text{eq}}$ regime. By also using the envelope of the j_1 spherical Bessel function, i.e. $j_1(x) \simeq 1/x$, we obtain:

$$\mathcal{T}_1(k) \simeq \frac{3}{(k\tau_0)^2} \sqrt{s_1} \left(\frac{k}{k_{\text{eq}}}\right). \quad (32)$$

In this regime, the neutrino free-streaming factor, \mathcal{T}_3 , is one (see Ref. [88] for more details). As such, we express the complete transfer function as:

$$\mathcal{T}^2(k) = \frac{9s_1}{k^2\tau_0^4 k_{\text{eq}}^2} \frac{\Omega_M^2}{\Omega_\Lambda^2}, \quad (33)$$

where in the $k \gg k_{\text{eq}}$ regime, the only relevant coefficient from Eq. 31 is s_1 . Inserting $\mathcal{T}^2(k)$ from Eq. 33 and $\mathcal{P}_T^{\text{prim}}(k)$ from Eq. 17 into Eq. 16 gives:

$$\Omega_{\text{gw}}(k) = \frac{3s_1}{4\tau_0^4 H_0^2 k_{\text{eq}}^2} \frac{\Omega_M^2}{\Omega_\Lambda^2} \cdot r A_s \left(\frac{k}{k_\star}\right)^{n_T}. \quad (34)$$

We can now connect the inflationary and PTA parameters via the GW spectral energy density. In particular, we equate $\Omega_{\text{gw}}(k)$ from Eq. 34 to $\Omega_{\text{gw}}^{\text{PTA}}(f)$ from Eq. 19. This first yields a relation between the tensor spectral index n_T and the spectral index γ :

$$n_T = 5 - \gamma. \quad (35)$$

Utilizing this relation and further equating the PTA and inflationary GW spectral energy densities gives a relation between the intrinsic-noise amplitude A and the inflationary parameters r and n_T :

$$A = \frac{\Omega_M}{\Omega_\Lambda} \sqrt{\frac{9s_1 A_s \gamma^2}{8\pi^2 \tau_0^4 k_{\text{eq}}^2}} \left(\frac{\gamma \Gamma^{-1}}{f_\star}\right)^{n_T/2} \sqrt{r}, \quad (36)$$

which, along with Eq. 35, will be our primary connection between the NANOGrav 15-year posteriors and the inflationary parameter space.

Since primordial GWs act like extra radiation as they propagate within the horizon, we must consider their contribution to the radiation energy density of the early universe. This contribution has effects on Big Bang Nucleosynthesis (BBN), which provides an important constraint [79, 89, 93–95]:

$$\Delta N_{\text{eff}}^{\text{gw}} \simeq \frac{h_0^2}{5.6 \times 10^{-6}} \int_{f_{\text{min}}}^{f_{\text{max}}} d(\ln f) \Omega_{\text{gw}}(f). \quad (37)$$

The term $\Delta N_{\text{eff}}^{\text{gw}}$ represents the GW contribution to the effective number of relativistic species, ΔN_{eff} , and is constrained by BBN and CMB probes to $\Delta N_{\text{eff}}^{\text{gw}} \lesssim 0.4$ at a 2σ upper limit [64, 96, 97]. The frequencies f_{min} and f_{max} depend on the epoch of BBN and the reheating temperature T_{rh} , respectively. Only modes within the horizon at the time of BBN can contribute to ΔN_{eff} , meaning f_{min} will be determined by the size of the horizon at the beginning of BBN. This scale corresponds to

10^{-12} Hz, but in actuality, modes will need to begin oscillating to contribute to the radiation energy density. As such, we will set $f_{\min} = 10^{-10}$ Hz [95]. Assuming instantaneous reheating after inflation ends, the upper limit f_{\max} is roughly proportional to the reheating temperature T_{rh} . We benchmark this proportionality with GUT-scale reheating, where $T_{\text{rh}} \simeq 10^{15}$ GeV corresponds to $f_{\max} \simeq 10^8$ Hz.

IV. DATA AND METHODS

As mentioned above, the NANOGrav collaboration reported evidence for a stochastic signal that was correlated among 67 pulsars from a 15-year pulsar-timing dataset [20]. Importantly, the correlations follow the Hellings-Downs pattern expected for a stochastic GW background, pointing to a true GW origin for the source [17]. The NANOGrav collaboration performed extensive analysis on this 15-year pulsar-timing dataset, and constructed a joint posterior probability distribution of the intrinsic-noise amplitude A and the spectral index γ in a Hellings-Downs power-law model [20]. This posterior distribution, shown in Fig. 1b (the blue contours using $f_{\text{ref}} = 1 \text{ yr}^{-1}$) of Ref. [20], will be used as the primary signal for our PTA data.

To constrain the region of inflationary parameter space ($\log_{10} r$ vs. n_T space) corresponding to the NANOGrav posterior, a grid scan could be performed using Eq. 35-36. In fact, this method was initially utilized to identify the general characteristics of the contours in inflationary parameter space. However, we choose a more versatile technique and perform a Bayesian analysis by using a Markov Chain Monte Carlo (MCMC) algorithm to map out the region of inflationary parameter space. We'll use the Metropolis-Hastings algorithm to dictate the sampling of the NANOGrav posterior, and we'll evaluate the convergence of the MCMC chains using the Gelman-Rubin parameter $R - 1$, requiring $R - 1 < 10^{-3}$ for a run [98].

The NANOGrav posterior will serve as the likelihood for the MCMC run. We find that the NANOGrav posterior is well approximated as a multivariate Gaussian distribution over $\log_{10} A$ and γ . This Gaussian can be described via its mean vector $\boldsymbol{\mu}_N$ and its covariance matrix $\boldsymbol{\Sigma}_N$:

$$\boldsymbol{\mu}_N \simeq [3.25, -14.19] \quad (38)$$

$$\boldsymbol{\Sigma}_N \simeq \begin{bmatrix} 0.129 & -0.045 \\ -0.045 & 0.0191 \end{bmatrix}. \quad (39)$$

The joint posterior distribution from this approximation is shown in Fig. 2. Using this distribution, the log-likelihood for the MCMC runs is:

$$\ln \mathcal{L}(\boldsymbol{\theta}) = -\frac{(\mathbf{x}(\boldsymbol{\theta}) - \boldsymbol{\mu}_N)^T \boldsymbol{\Sigma}_N^{-1} (\mathbf{x}(\boldsymbol{\theta}) - \boldsymbol{\mu}_N)}{2}, \quad (40)$$

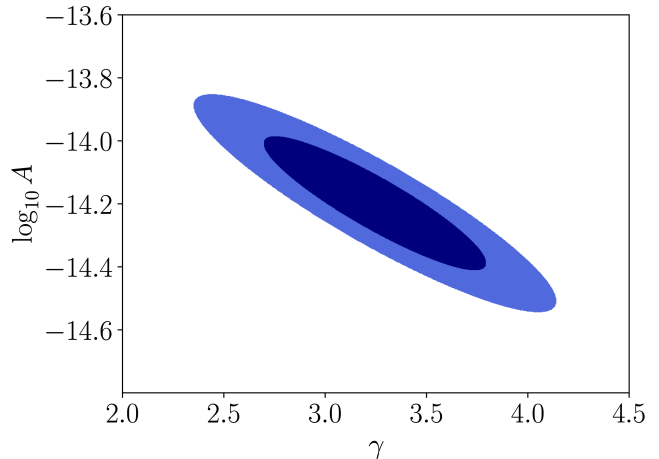


FIG. 2. The 2D joint posterior probability distribution for the logarithm of the intrinsic-noise amplitude $\log_{10} A$ and the spectral index γ , using a multivariate Gaussian distribution to approximate the NANOGrav 15-year posterior. Comparing this distribution with Fig. 1b of Ref. [20] shows excellent agreement between the two, confirming the validity of this approximation.

where $\mathbf{x}(\boldsymbol{\theta}) \equiv [\log_{10} A(\boldsymbol{\theta}), \gamma(\boldsymbol{\theta})]$ is a vector of the dependent parameters, $\boldsymbol{\theta}$ is a vector of the independent parameters, which we take to be $\boldsymbol{\theta} = [r, n_T]$, and T denotes the transpose operation. The functions $\log_{10} A(\boldsymbol{\theta})$ and $\gamma(\boldsymbol{\theta})$ used to calculate $\mathbf{x}(\boldsymbol{\theta})$ are given by Eq. 36 and Eq. 35, respectively. Technically, $\boldsymbol{\theta}$ should include all cosmological parameters relevant to an inflationary GW, i.e. $H_0, A_s, \Omega_m, \Omega_r, n_T$ and r , but we simply fix all but n_T and r to their *Planck* 2018 values [64].

This likelihood in Eq. 40 is supplied to the cosmological sampler *MontePython*, which we utilize to perform the MCMC runs [99, 100]. We also choose to work with $\log_{10} r$ instead of r , as the magnitude of r is still unknown. We impose flat, wide priors on both n_T and $\log_{10} r$, and impose a hard prior of $\log_{10} r < -1.44$ corresponding to the 2σ constraint $r < 0.036$ from analysis of *Planck*, WMAP, BICEP3, and *Keck* data [101].

V. RESULTS

We perform MCMC runs as described in the previous section to identify the region of inflationary parameter space corresponding to the NANOGrav joint A - γ posterior probability distribution using the model of GR and the model of MG. Specifically, we set $s_1 = 4.16$ for the GR case and $s_1 = 1.3 \cdot 10^6$ in the MG case in Eq. 36, which affects the likelihood in Eq. 40 as described in Section IV. The results of these MCMC runs are shown in Fig. 3, where the color scheme matches that of Fig. 1: i.e. blue for the GR model and red for the MG model.

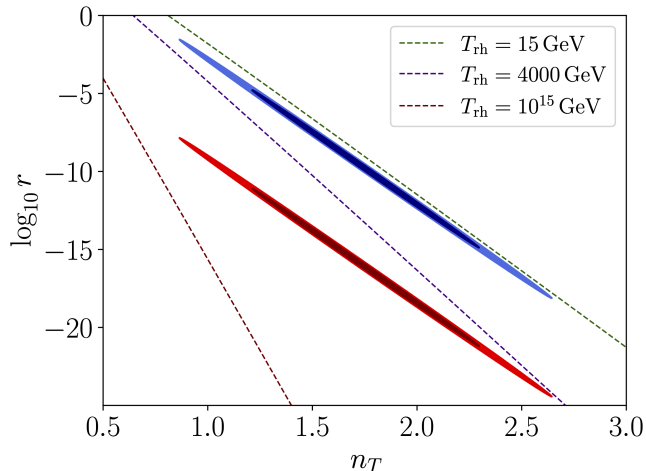


FIG. 3. The 2D joint posterior probability distribution for the logarithm of the tensor-to-scalar ratio r and the tensor spectral index n_T , generated by mapping the joint posterior probability distribution from Fig. 2 via MCMC runs. The dashed lines are produced by fixing $\Delta N_{\text{eff}}^{\text{gw}} = 0.4$ in Eq. 37, and setting the integral upper bound f_{max} to the a value corresponding to a particular reheating temperature T_{rh} . The region to the left of a dashed line is acceptable under that value of the reheating temperature.

Looking at the 1σ contours, we find that:

$$n_T = 1.75 \pm 0.54 \quad (41)$$

$$\log_{10} r = -9.83 \pm 5.05, \quad (42)$$

for the GR model, while:

$$n_T = 1.75 \pm 0.54 \quad (43)$$

$$\log_{10} r = -16.14 \pm 5.05, \quad (44)$$

for the MG model. Observe that the mean of $\log_{10} r$ is lower in the MG model, as a result of the different value of s_1 . The 1σ and 2σ contours for the GR and MG models both show a negative correlation between n_T and $\log_{10} r$, which is expected. Recalling the form of Eq. 17, we see that higher values of n_T can be compensated by lower values of r , and vice-versa. This behavior is independent of the choice of s_1 , and thus appears for both the GR and MG models. The relationship between γ and n_T , given by Eq. 35, is also independent of s_1 , which explains why the range of values for n_T is shared for both models.

Since the range of n_T for both models is much greater than zero, we characterize the spectrum as strongly blue; this strongly blue spectrum presents challenges for an inflationary justification. First, observe that this spectrum violates the consistency relation discussed in Section II, which requires a slightly red spectrum. This relation only applied to the simple single-field slow-roll inflationary model, meaning other models may suffice. Second, reconsider Eq. 18 and observe that $n_T = 1.75$ would require $w = -\frac{17}{3}$, which difficult to reach theoretically due to it being deep within the phantom regime.

However, previous works have investigated how double-field inflation [102–105], axion inflation [31, 106, 107], or quintessential inflation [108–110] could produce a sufficiently blue spectrum to conform with the NANOGrav signal. Other mechanisms within previous models can also be adequate, such as scalar induced GWs [111] or the removal of the Bunch-Davies initial condition [30], both of which utilize single-field inflation. As such, the strongly blue spectrum can be justified, but with some difficulty.

We now turn our attention to the inflationary parameter $\log_{10} r$ in Fig. 3, for which we see that the range of values of $\log_{10} r$ for the MG model is lower than that of the GR model. The significance of this comes from its effect on the fixed reheating temperature isocontours shown as dashed lines in Fig. 3. These lines come from the BBN bound in Eq. 37, using $\Delta N_{\text{eff}}^{\text{gw}} = 0.4$ (see Section III), and setting f_{max} based on the chosen value of the reheating temperature T_{rh} . The region to the left of a particular dashed line represents the region of n_T - r parameter space that agrees with the chosen reheating temperature T_{rh} according to the BBN integral from Eq. 37. The three reheating temperatures considered for Fig. 3 are $T_{\text{rh}} \simeq 15$ GeV, $T_{\text{rh}} \simeq 4000$ GeV, and $T_{\text{rh}} \simeq 10^{15}$ GeV. The former two temperatures have been chosen to constrain the GR and MG models respectively, while the latter temperature is the GUT-scale reheating temperature, used in Section III to calibrate the proportionality between f_{max} and T_{rh} . Importantly, the reheating temperature for the MG model is higher than reheating temperature for the GR model, due to the lower mean value of $\log_{10} r$ for the MG model. These reheating scales are quite low, but not excluded from possibility, as the reheating temperature can be as low as 5 MeV according to previous probes [112]. However, similar to a bluer spectrum in n_T , a lower reheating temperature is harder to motivate theoretically. Hence, although both MG and GR models are technically viable, the MG model is less cumbersome to motivate due to its higher reheating temperature.

Overall, an inflationary interpretation of the NANOGrav signal remains challenging, as shown in other works [23, 27–31, 33]. The inclusion of a MG model relaxes the difficulty of explaining the low reheating temperature, but the strongly blue spectrum is still tough to motivate. The possibility of an inflationary interpretation in the GR model is poor due to constraints from both the low reheating temperature and the blue spectrum, while the MG model’s interpretation is slightly better due to its higher reheating temperature.

VI. CONCLUSIONS

In this work, we’ve considered how the recently released NANOGrav 15-year dataset could be interpreted as an inflationary GW background by using MTMG with a step function mass instead of standard GR. Us-

ing a modified EoM, a result of MTMG, we've calculated a transfer function that describes the evolution of GW modes across the universe's history. This transfer function was then used to derive a new GW spectral energy density, which would serve at the connecting point between the inflationary theory and the PTA signal from NANOGrav. As such, we were able to map the NANOGrav A - γ joint posterior probability distribution onto the n_T - r inflationary parameter space, by using a MCMC scan. The relevant regions of inflationary parameter space are shown in Fig. 3, which shows 1σ and 2σ contours for both the GR and MG models. Analyzing this figure, we find that an inflationary interpretation would require a strongly blue spectrum, with a relatively low reheating temperature. Though both of these constraints are theoretically viable, motivating both of them remains challenging. Importantly, the MG model permits a higher reheating temperature than the GR model, slightly relaxing the difficulty of an inflationary interpretation in the MG case.

As discussed in Section III, a specific graviton mass and cutoff time were selected in our work prior to calculating the transfer function for MG via numerical integration. Future work may consider different ranges for graviton mass, or later cutoff times, to evaluate how each of these

affect the transfer function. In particular, it may be fruitful to determine what ranges for the graviton mass and cutoff time within previously studied bounds would lead to the most tenable inflationary interpretation.

A. Data Availability

The NANOGrav 15-year Data Set used in this paper is available from NANOGrav [113]. Source code required to reproduce the analysis and figures in this paper are available in the GitHub repository [114].

B. Acknowledgements

We'd like to thank Murman Gurgenzidze and Sayan Mandal for helpful discussions, as well as Chris Choi and Jacob Magallanes for useful cross-checks of GW evolution in the MTMG model. Furthermore, we thank Sunny Vagnozzi for assistance with the MCMC runs. TK acknowledges partial support from the NASA Astrophysics Theory Program (ATP) Award 80NSSC22K0825 and National Science Foundation (NSF) award AST2408411.

-
- [1] A. A. Starobinsky, *JETP Lett.* **30**, 682 (1979).
 - [2] A. H. Guth, *Phys. Rev. D* **23**, 347 (1981).
 - [3] A. D. Linde, *Phys. Lett. B* **108**, 389 (1982).
 - [4] L. P. Grishchuk, *Zh. Eksp. Teor. Fiz.* **67**, 825 (1974).
 - [5] M. Maggiore, *Gravitational Waves: Volume 2: Astrophysics and Cosmology* (Oxford University Press, Oxford, 2018).
 - [6] C. Caprini and D. G. Figueroa, *Class. Quant. Grav.* **35**, 163001 (2018).
 - [7] J. P. W. Verbiest, M. Bailes, W. A. Coles, G. B. Hobbs, W. van Straten, D. J. Champion *et al.*, *Monthly Notices of the Royal Astronomical Society* **400**, 951–968 (2009).
 - [8] M. V. Sazhin, *Sov. Astron. J. (Astron. Zhur.* **55**, 65 (1978).
 - [9] S. L. Detweiler, *Astrophys. J.* **234**, 1100 (1979).
 - [10] G. Agazie, A. Anumalapudi, A. M. Archibald, Z. Arzoumanian, P. T. Baker, B. Bécsy *et al.*, *The Astrophysical Journal Letters* **951**, L8 (2023).
 - [11] EPTA Collaboration, J. Antoniadis, S. Babak, A. S. Bak Nielsen, C. G. Bassa, A. Berthreau *et al.*, *Astron. Astrophys.* **678**, A48 (2023).
 - [12] J. Antoniadis *et al.* (EPTA, InPTA:), *Astron. Astrophys.* **678**, A50 (2023).
 - [13] J. Antoniadis *et al.* (EPTA, InPTA), *Astron. Astrophys.* **678**, A49 (2023).
 - [14] A. Zic, D. J. Reardon, A. Kapur, G. Hobbs, R. Mandow, M. Curyło *et al.*, *PASA* **40**, e049 (2023).
 - [15] D. J. Reardon *et al.*, *Astrophys. J. Lett.* **951**, 10.3847/2041-8213/acdd02 (2023).
 - [16] H. Xu *et al.*, *Res. Astron. Astrophys.* **23**, 075024 (2023).
 - [17] R. w. Hellings and G. s. Downs, *Astrophys. J. Lett.* **265**, L39 (1983).
 - [18] J. D. Romano and N. J. Cornish, *Living Rev. Rel.* **20**, 2 (2017).
 - [19] N. Yunes and X. Siemens, *Living Reviews in Relativity* **16**, 9 (2013).
 - [20] G. Agazie *et al.* (NANOGrav), *Astrophys. J. Lett.* **951**, L8 (2023).
 - [21] L. Bian, S. Ge, J. Shu, B. Wang, X.-Y. Yang and J. Zong, *Phys. Rev. D* **109**, L101301 (2024).
 - [22] A. Afzal *et al.* (NANOGrav), *Astrophys. J. Lett.* **951**, L11 (2023), [Erratum: *Astrophys. J. Lett.* 971, L27 (2024), Erratum: *Astrophys. J.* 971, L27 (2024)].
 - [23] S. Vagnozzi, *Mon. Not. Roy. Astron. Soc.* **502**, L11 (2021).
 - [24] A. S. Sakharov, Y. N. Eroshenko and S. G. Rubin, *Phys. Rev. D* **104**, 043005 (2021).
 - [25] G. Lazarides, R. Maji and Q. Shafi, *Phys. Rev. D* **104**, 095004 (2021).
 - [26] A. Brandenburg and R. Sharma, *Astrophys. J.* **920**, 26 (2021).
 - [27] S. Vagnozzi, *JHEAp* **39**, 81 (2023).
 - [28] S. D. Odintsov, V. K. Oikonomou, I. Giannakoudi, F. P. Fronimos and E. C. Lympriadiou, *Symmetry* **15**, 1701 (2023).
 - [29] S. Choudhury, A. Karde, S. Panda and M. Sami, (2023).
 - [30] S. Choudhury, *Eur. Phys. J. C* **84**, 278 (2024).
 - [31] X. Niu and M. H. Rahat, *Phys. Rev. D* **108**, 115023 (2023).
 - [32] S. Datta and R. Samanta, *Phys. Rev. D* **108**, L091706 (2023).
 - [33] J.-Q. Jiang, Y. Cai, G. Ye and Y.-S. Piao, *JCAP* **05** (5), 004.

- [34] D. G. Figueroa, M. Pieroni, A. Ricciardone and P. Simakachorn, *Phys. Rev. Lett.* **132**, 171002 (2024).
- [35] D. Borah, S. Jyoti Das and R. Samanta, *JCAP* **03** (3), 031.
- [36] G. Lazarides, R. Maji, A. Moursy and Q. Shafi, *JCAP* **03** (3), 006.
- [37] C. Fu, J. Liu, X.-Y. Yang, W.-W. Yu and Y. Zhang, *Phys. Rev. D* **109**, 063526 (2024).
- [38] M. Correa, M. R. Gangopadhyay, N. Jaman and G. J. Mathews, *Phys. Rev. D* **109**, 063539 (2024).
- [39] Z.-C. Chen and L. Liu, *JCAP* **06** (6), 028.
- [40] H. Firouzjahi and A. Talebian, *JCAP* **10** (10), 032.
- [41] Z. Arzoumanian *et al.* (NANOGrav), *Astrophys. J. Lett.* **905**, L34 (2020).
- [42] Y. Akrami *et al.* (Planck), *Astron. Astrophys.* **641**, A10 (2020).
- [43] C. de Rham, J. T. Deskins, A. J. Tolley and S.-Y. Zhou, *Rev. Mod. Phys.* **89**, 025004 (2017).
- [44] M. Fierz and W. Pauli, *Proc. Roy. Soc. Lond. A* **173**, 211 (1939).
- [45] G. D'Amico, C. de Rham, S. Dubovsky, G. Gabadadze, D. Pirtskhalava and A. J. Tolley, *Phys. Rev. D* **84**, 124046 (2011).
- [46] V. I. Zakharov, *JETP Lett.* **12**, 312 (1970).
- [47] H. van Dam and M. J. G. Veltman, *Nucl. Phys. B* **22**, 397 (1970).
- [48] A. I. Vainshtein, *Phys. Lett. B* **39**, 393 (1972).
- [49] D. G. Boulware and S. Deser, *Phys. Rev. D* **6**, 3368 (1972).
- [50] C. de Rham and G. Gabadadze, *Phys. Rev. D* **82**, 044020 (2010).
- [51] C. de Rham, G. Gabadadze and A. J. Tolley, *Phys. Rev. Lett.* **106**, 231101 (2011).
- [52] S. F. Hassan and R. A. Rosen, *Phys. Lett. B* **702**, 90 (2011).
- [53] A. E. Gumrukcuoglu, C. Lin and S. Mukohyama, *JCAP* **03** (3), 006.
- [54] A. E. Gumrukcuoglu, S. Kuroyanagi, C. Lin, S. Mukohyama and N. Tanahashi, *Class. Quant. Grav.* **29**, 235026 (2012).
- [55] C. de Rham, *Living Rev. Rel.* **17**, 7 (2014).
- [56] D. Blas, C. Deffayet and J. Garriga, *Phys. Rev. D* **76**, 104036 (2007).
- [57] V. A. Rubakov and P. G. Tinyakov, *Phys. Usp.* **51**, 759 (2008).
- [58] D. Blas, D. Comelli, F. Nesti and L. Pilo, *Phys. Rev. D* **80**, 044025 (2009).
- [59] V. Rubakov, *arXiv e-prints*, hep-th/0407104 (2004).
- [60] A. De Felice and S. Mukohyama, *Phys. Lett. B* **752**, 302 (2016).
- [61] A. De Felice and S. Mukohyama, *JCAP* **04** (4), 028.
- [62] A. Higuchi, *Nucl. Phys. B* **282**, 397 (1987).
- [63] T. Fujita, S. Kuroyanagi, S. Mizuno and S. Mukohyama, *Phys. Lett. B* **789**, 215 (2019).
- [64] N. Aghanim *et al.* (Planck), *Astron. Astrophys.* **641**, A6 (2020), [Erratum: *Astron. Astrophys.* 652, C4 (2021)].
- [65] C. Choi, J. Magallanes, M. Gurgunidze and T. Kahniashvili, *Phys. Rev. D* **110**, 063525 (2024).
- [66] G. D'Amico, G. Gabadadze, L. Hui and D. Pirtskhalava, *Phys. Rev. D* **87**, 064037 (2013).
- [67] T. Kahniashvili, A. Kar, G. Lavrelashvili, N. Agarwal, L. Heisenberg and A. Kosowsky, *Phys. Rev. D* **91**, 041301 (2015), [Erratum: *Phys. Rev. D* 100, 089902 (2019)].
- [68] A. De Felice and S. Mukohyama, *Phys. Lett. B* **728**, 622 (2014).
- [69] A. De Felice, A. Emir Gümrukçüoğlu and S. Mukohyama, *Phys. Rev. D* **88**, 124006 (2013).
- [70] G. D'Amico, G. Gabadadze, L. Hui and D. Pirtskhalava, *Class. Quant. Grav.* **30**, 184005 (2013).
- [71] R. Gannouji, M. W. Hossain, M. Sami and E. N. Saridakis, *Phys. Rev. D* **87**, 123536 (2013).
- [72] S. Mukohyama, *JCAP* **12** (12), 011.
- [73] R. Abbott *et al.* (LIGO Scientific, Virgo, KAGRA), *Phys. Rev. Lett.* **126**, 241102 (2021).
- [74] R. Abbott *et al.* (LIGO Scientific, VIRGO, KAGRA), *arXiv e-prints*, arXiv:2112.06861 (2021).
- [75] Y.-M. Wu, Z.-C. Chen and Q.-G. Huang, *Phys. Rev. D* **107**, 042003 (2023).
- [76] S. Wang and Z.-C. Zhao, *Phys. Rev. D* **109**, L061502 (2024).
- [77] A. De Felice, S. Mukohyama and M. C. Pookkillath, *Phys. Rev. D* **106**, 084050 (2022).
- [78] A. De Felice, S. Kumar, S. Mukohyama and R. C. Nunes, *JCAP* **04** (4), 013.
- [79] M. Maggiore, *Phys. Rept.* **331**, 283 (2000).
- [80] S. Kuroyanagi, T. Chiba and N. Sugiyama, *Phys. Rev. D* **79**, 103501 (2009).
- [81] S. Kuroyanagi, T. Chiba and N. Sugiyama, *Phys. Rev. D* **83**, 043514 (2011).
- [82] S. Kuroyanagi, K. Nakayama and S. Saito, *Phys. Rev. D* **84**, 123513 (2011).
- [83] E. J. Copeland, E. W. Kolb, A. R. Liddle and J. E. Lidsey, *Phys. Rev. Lett.* **71**, 219 (1993).
- [84] Y.-S. Piao and Y.-Z. Zhang, *Phys. Rev. D* **70**, 063513 (2004).
- [85] L. Shao, N. Wex and S.-Y. Zhou, *Phys. Rev. D* **102**, 024069 (2020).
- [86] L. S. Finn and P. J. Sutton, *Phys. Rev. D* **65**, 044022 (2002).
- [87] B. P. Abbott *et al.* (LIGO Scientific, Virgo, Fermi-GBM, INTEGRAL), *Astrophys. J. Lett.* **848**, L13 (2017).
- [88] W. Zhao and Y. Zhang, *Phys. Rev. D* **74**, 043503 (2006).
- [89] S. Kuroyanagi, T. Takahashi and S. Yokoyama, *JCAP* **02** (2), 003.
- [90] R. Durrer and T. Kahniashvili, *Helv. Phys. Acta* **71**, 445 (1998).
- [91] S. Weinberg, *Phys. Rev. D* **69**, 023503 (2004).
- [92] M. S. Turner, M. J. White and J. E. Lidsey, *Phys. Rev. D* **48**, 4613 (1993).
- [93] L. A. Boyle and A. Buonanno, *Phys. Rev. D* **78**, 043531 (2008).
- [94] W. Giarè, M. Forconi, E. Di Valentino and A. Melchiorri, *Mon. Not. Roy. Astron. Soc.* **520**, 2 (2023).
- [95] G. Cabass, L. Pagano, L. Salvati, M. Gerbino, E. Giusarma and A. Melchiorri, *Phys. Rev. D* **93**, 063508 (2016).
- [96] T. Hsyu, R. J. Cooke, J. X. Prochaska and M. Bolte, *Astrophys. J.* **896**, 77 (2020).
- [97] S. Aiola *et al.* (ACT), *JCAP* **12** (12), 047.
- [98] A. Gelman and D. B. Rubin, *Statistical Science* **7**, 457 (1992).
- [99] T. Brinckmann and J. Lesgourgues, *Phys. Dark Univ.* **24**, 100260 (2019).
- [100] B. Audren, J. Lesgourgues, K. Benabed and S. Prunet, *JCAP* **1302** (2), 001.

- [101] P. A. R. Ade *et al.* (BICEP, Keck), [Phys. Rev. Lett.](#) **127**, 151301 (2021).
- [102] F. C. Adams and K. Freese, [Phys. Rev. D](#) **43**, 353 (1991).
- [103] A. Ashoorioon, [Phys. Lett. B](#) **747**, 446 (2015).
- [104] A. Ashoorioon, K. Rezazadeh and A. Rostami, [Phys. Lett. B](#) **835**, 137542 (2022).
- [105] S. Tsujikawa, D. Parkinson and B. A. Bassett, [Phys. Rev. D](#) **67**, 083516 (2003).
- [106] L. McAllister, E. Silverstein and A. Westphal, [Phys. Rev. D](#) **82**, 046003 (2010).
- [107] R. Flauger, L. McAllister, E. Pajer, A. Westphal and G. Xu, [JCAP](#) **06** (6), 009.
- [108] B. Das, N. Jaman and M. Sami, [Phys. Rev. D](#) **108**, 103510 (2023).
- [109] P. J. E. Peebles and A. Vilenkin, [Phys. Rev. D](#) **59**, 063505 (1999).
- [110] M. Sami and V. Sahni, [Phys. Rev. D](#) **70**, 083513 (2004).
- [111] L. Frosina and A. Urbano, [Phys. Rev. D](#) **108**, 103544 (2023).
- [112] P. F. de Salas, M. Lattanzi, G. Mangano, G. Miele, S. Pastor and O. Pisanti, [Phys. Rev. D](#) **92**, 123534 (2015).
- [113] T. N. Collaboration, [10.5281/zenodo.8423265](#) (2023).
- [114] V. Kenjale, [nanograv15-mg-paper](#) (2024).